Journal of Power Sources 195 (2010) 1510–1515

Contents lists available at ScienceDirect

Journal of Power Sources

journal homepage: www.elsevier.com/locate/jpowsour

Short communication

On the $LiNi_{0.2}Mn_{0.2}Co_{0.6}O_2$ positive electrode material

Yassine Bentaleb[a], Ismael Saadoune[a,*], Kenza Maher[a], Latifa Saadi[b], Kenjiro Fujimoto[c], Shigeru Ito[c]

[a] ECME, Faculté des Sciences et Techniques Marrakech, University Cadi Ayyad, BP549, Av. A. Khattabi, 40000 Marrakech, Morocco
[b] EVAR-MIMAS, Faculté des Sciences et Techniques Marrakech, University Cadi Ayyad, BP549, Av. A. Khattabi, 40000 Marrakech, Morocco
[c] Department of Pure and Applied Chemistry, Faculty of Science and Technology, Tokyo University of Science, Yamazaki 2461, Noda, Chiba 278-8510, Japan

ARTICLE INFO

Article history:
Received 28 May 2009
Received in revised form 1 September 2009
Accepted 10 September 2009
Available online 20 September 2009

Keywords:
Cathode material
Lithium batteries
Rate capability
Magnetic properties

ABSTRACT

Layered $LiNi_{0.2}Mn_{0.2}Co_{0.6}O_2$ phase, belonging to a solid solution between $LiNi_{1/2}Mn_{1/2}O_2$ and $LiCoO_2$ most commercialized cathodes, was prepared via the combustion method at 900 °C for a short time (1 h). Structural, electrochemical and magnetic properties of this material were investigated. Rietveld analysis of the XRD pattern shows this compound as having the α-$NaFeO_2$ type structure (S.G. R-3m; $a = 2.8399(2)$ Å; $c = 14.165(1)$ Å) with almost none of the well-known Li/Ni cation disorder. SQUID measurements clearly indicate that the studied compound consists of Ni^{2+}, Co^{3+} and Mn^{4+} ions in the crystal structure. X-ray analysis of the chemically delithiated $Li_xNi_{0.2}Mn_{0.2}Co_{0.6}O_2$ phases reveals that the rhombohedral symmetry was maintained during Li-extraction, confirmed by the monotonous variation of the potential–composition curve of the $Li//Li_xNi_{0.2}Mn_{0.2}Co_{0.6}O_2$ cell. $LiNi_{0.2}Mn_{0.2}Co_{0.6}O_2$ cathode has a discharge capacity of ~160 mAh g^{-1} in the voltage range 2.7–4.3 V corresponding to the extraction/insertion of 0.6 lithium ion with very low polarization. It exhibits a stable capacity on cycling and good rate capability in the rate range 0.2–2 C. The almost 2D structure of this cathode material, its good electrochemical performances and its relatively low cost comparing to $LiCoO_2$, make this material very promising for applications.

1. Introduction

Recently, layered $Li(Ni_{0.5}Mn_{0.5})O_2$ and $Li(Ni_{1/3}Mn_{1/3}Co_{1/3})O_2$ have received much attention as a promising alternative to the commercialized $LiCoO_2$ cathode for lithium ion batteries [1–4]. Indeed, the high cost, toxicity, limited rate capability and safety concerns of the conventional $LiCoO_2$ material remain to be problematic to develop the lithium ion battery technology for electric and hybrid vehicles. In the two former layered oxides, it has been demonstrated that Mn^{4+} ions are electrochemically inactive during the cycling process. They provide significant structural stability during the electrochemical cycling. The redox activity takes place mainly in the nickel center and the $Ni^{2+}/Ni^{3+}/Ni^{4+}$ are believed to be involved during the lithium extraction/insertion reactions [5].

It should be noticed that $Li(Ni_{0.5}Mn_{0.5})O_2$ and $Li(Ni_{1/3}Mn_{1/3}Co_{1/3})O_2$ electrode materials have the same Ni^{2+}/Mn^{4+} ratio in their starting state. They could then be considered as members of the $Li(Ni_xMn_xCo_{1-2x})O_2$ solid solution with x equal respectively to 1/2 and 1/3. Ohzuku and Makimura considered that $Li(Ni_xMn_xCo_{1-2x})O_2$ system looks like a simple solid solution in the $LiNiO_2$–$LiMnO_2$–$LiCoO_2$ ternary diagram [6]. But, the oxidation states of the transition metal ions in $Li(Ni_xMn_xCo_{1-2x})O_2$ differ from those of the three end members. Thus, we could consider that $Li(Ni_xMn_xCo_{1-2x})O_2$ $(0 \le x \le 1/2)$ is rather a solid solution in the $Li(Ni_{0.5}Mn_{0.5})O_2$–$LiCoO_2$ binary system.

Many compositions within this solid solution were investigated by several authors. Li et al. reported that $LiNi_{0.4}Co_{0.2}Mn_{0.4}O_2$ cathode material exhibits an excellent electrochemical performances and storage stability [7]. It delivers a first discharge capacity of 204.8 mAh g^{-1}. While Myung et al. showed that the electrochemical performances of the $Li(Ni_{0.5}Mn_{0.5})_{1-x}Co_xO_2$ system were improved by increasing the Co content which reduce the well-known Li^+/Ni^{2+} disorder [8]. Furthermore, it has been demonstrated that the rate capability and diffusion coefficient decrease with x. Nevertheless, almost all studied compounds were prepared at relatively high temperature (more than 900 °C) and for a long annealing time. With the aim to prepare a new cathode material in the $Li(Ni_xMn_xCo_{1-2x})O_2$ $(0 \le x \le 1/2)$ system which contains the best positive electrode materials to date, we have investigated this solid solution and study the evolution of the structural and electrochemical performances with the Ni^{2+} and Mn^{4+} amount. Here we started by the $LiNi_{0.2}Mn_{0.2}Co_{0.6}O_2$ phase which has been prepared by the combustion method at relatively low temperature and for a short annealing time in order to reduce the Li/Ni disorder. The physical and electrochemical properties of the prepared material have been thoroughly investigated.

* Corresponding author. Tel.: +212 661 48 64 64; fax: +212 524 43 31 70.
E-mail address: saadoune1@yahoo.fr (I. Saadoune).

0378-7753/$ – see front matter © 2009 Elsevier B.V. All rights reserved.
doi:10.1016/j.jpowsour.2009.09.026

2. Experimental

A typical combustion synthesis of $LiNi_{0.2}Mn_{0.2}Co_{0.6}O_2$ with sucrose as a fuel was performed using the following way: stoichiometric amounts of nickel, cobalt and manganese nitrates were used as starting materials, while 5% excess of lithium nitrate were used in order to compensate for the possible lithium loss during high temperature annealing. These salts were dissolved in an aqueous solution simultaneously with sucrose and homogenized by a magnetic stirrer. It is important to note that when the stoichiometric sucrose/nitrate mixture is used, a violent explosion occurs. To avoid it, the sucrose/nitrate molar ratio was optimized to be equal to 0.67. The mixture was heated at about 120 °C for 1 h, and when dried it starts to swell up due to the evaporation of gases generated during the thermolysis of the reagents, giving way to a foamy mass. After a few minutes, the mass starts to burn up spontaneously without flame.

A portion of the as-prepared material was taken for the coupled TG-DTA thermal analysis in order to understand the decomposition behaviour and to determine the sintering temperature of $LiNi_{0.2}Mn_{0.2}Co_{0.6}O_2$ compound. Thermal analysis was carried out under air up to 1000 °C at a heating rate of 5 °C min^{-1} by using a Setaram.

Chemical extraction of lithium was carried out by stirring the $LiNi_{0.2}Mn_{0.2}Co_{0.6}O_2$ powder with an acetonitrile solution of the oxidizer NO_2BF_4 for 24 h under argon atmosphere, followed by washing the obtained products with acetonitrile.

The particles morphology was observed by scanning electron microscopy using HRSEM LEO 1550 equipment.

Powder X-ray diffraction patterns were collected using a Siemens D5000 diffractometer (Cu Kα radiation). The lattice parameters and cation distributions were refined by the Rietveld method using the Fullprof program [9].

The magnetic properties of $LiNi_{0.2}Mn_{0.2}Co_{0.6}O_2$ sample have been studied with a superconducting quantum interference device (SQUID) from Quantum Design. The susceptibility was measured in a magnetic field of 10,000 Oe on cooling sample from 300 to 2 K. The magnetization curves were measured in magnetic fields from −70,000 to 70,000 Oe.

The electrochemical measurements were performed using a Swagelock type cell. Positive electrode laminates from the oxide powders were prepared by coating a mixture of 85 wt% oxide, 10 wt% acetylene black and 5 wt% PVDF binder on a 30 μm Al foil. Lithium foil was used as anode while the liquid electrolyte was: 1 M $LiPF_6$ dissolved in ethylene carbonate–dimethyl carbonate (1:2 in volume) solution. The cells were assembled in an argon-filled glove box and tested at room temperature at 0.05–2 C-rates in the voltage range of 2.7–4.3 V. The cells were cycled using a constant charge–discharge current density for more than 40 cycles (current density equal to 28 mA g^{-1} at 0.1C rate).

3. Results and discussions

3.1. TG/DTA analysis

Fig. 1 shows the TG/DTA curves obtained from the mixture resulting from the combustion reaction. TG curve exhibits two significant weight losses located 110 and 450 °C corresponding to two endothermic phenomena. The first one corresponds to the loss of adsorbed water. The second weight loss can be ascribed to the decomposition of the residual nitrate precursors followed by the formation of $LiNi_{0.2}Mn_{0.2}Co_{0.6}O_2$ phase. This is confirmed by the absence of further weight loss in the 600–950 °C temperature range. For temperatures beyond 950 °C, less than 1% weight loss was detected while no significant DTA peak was observed. This is probably due to the start of the lithium

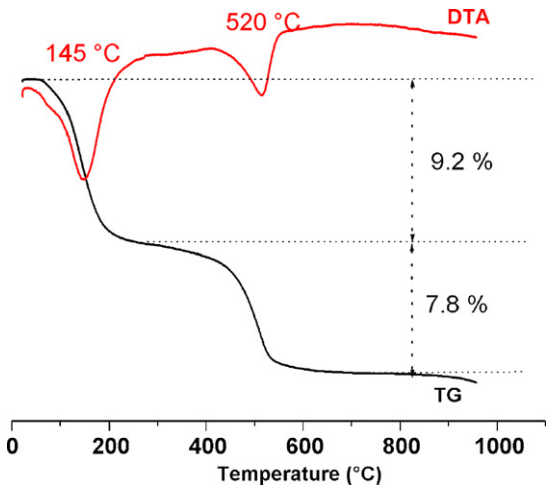

Fig. 1. DTA/TG curves of the $LiNi_{0.2}Mn_{0.2}Co_{0.6}O_2$ precursor resulting from the combustion reaction.

departure from the synthesised $LiNi_{0.2}Mn_{0.2}Co_{0.6}O_2$ layered compound.

Thus, according to these thermal analysis results, and tacking in account to high surface area of the mixture resulting from the combustion reaction, three synthesis conditions were chosen to achieve the $LiNi_{0.2}Mn_{0.2}Co_{0.6}O_2$ synthesis: (700 °C/12 h); (800 °C/12 h) and (900 °C/1 h).

3.2. X-ray diffraction

XRD analysis was used in order to find the optimal temperature for crystallization. Fig. 2 shows the thermal evolution of the XRD patterns at temperatures ranging from 700 to 900 °C. All the XRD patterns of the synthesised materials could be indexed in the rhombohedral system (S.G. R-3m) and no obvious impurities were detected. Nevertheless, a clear improvement of the crystallization state of the prepared materials with temperature was evidenced. The comparison of lattice parameters, $I_{(003)}/I_{(104)}$ integrated intensities ratio and the full width at half maximum (F_{WHM}) of the (0 0 3) peak intensity was given in Table 1.

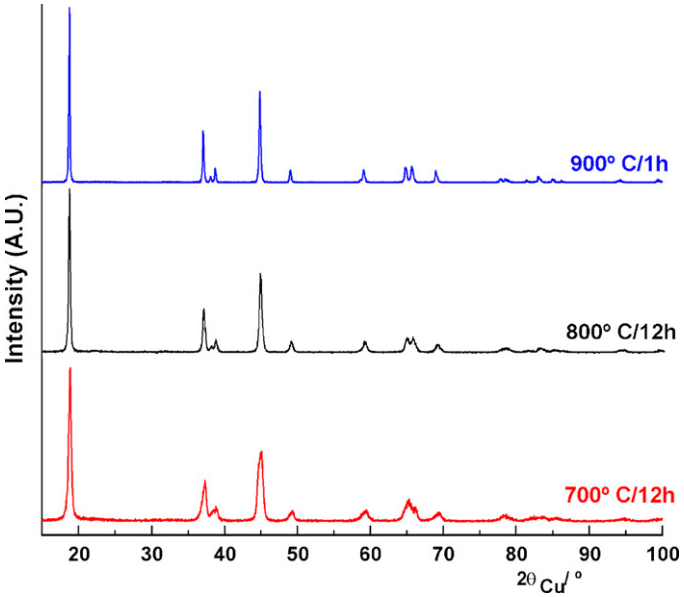

Fig. 2. X-ray diffraction patterns of $LiNi_{0.2}Mn_{0.2}Co_{0.6}O_2$ prepared at different conditions.

Table 1
Rietveld analysis results of the layered $LiNi_{0.2}Mn_{0.2}Co_{0.6}O_2$ samples synthesised at various temperatures.

Synthesis conditions	a (Å)	c (Å)	c/a	V (Å^3)	$I_{(003)}/I_{(104)}$	F_{WHM} (°)
700 °C/12 h	2.8341(3)	14.124(2)	4.9836	98.24	2.5	0.236
800 °C/12 h	2.8398(2)	14.161(2)	4.9866	98.90	2.1	0.207
900 °C/1 h	2.8399(2)	14.165(1)	4.9879	98.93	2.0	0.147

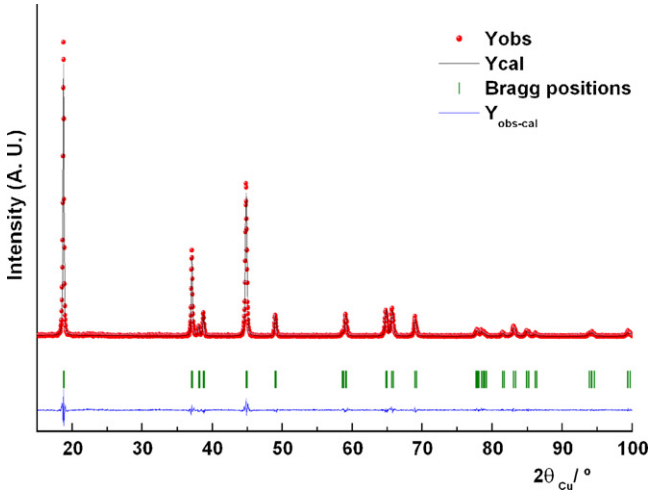

Fig. 3. Experimental XRD pattern and calculated from Rietveld program for $LiNi_{0.2}Mn_{0.2}Co_{0.6}O_2$.

The c/a ratio increases with temperature indicating the increase of the 2D character. The decrease of the F_{WHM} factor with increasing the annealing temperature is an indication of an improvement of the crystallization of the studied materials as confirmed by the particle sizes estimation from the Sherrer's formula [10]. Indeed, the particle size increases from 57 nm for the sample prepared at 700 °C, to more than 150 nm for that synthesised at 900 °C for 1 h.

The $I_{(003)}/I_{(104)}$ ratio of the three studied compound remains relatively high compared to the homologous layered oxide. A weak Li/Ni disorder is expected for these materials. This point has been studied more in detail by the Rietveld refinement method. Thus, one can conclude that in our case, the best synthesis condition of $LiNi_{0.2}Mn_{0.2}Co_{0.6}O_2$ positive electrode material were 900 °C for 1 h and the following characterizations will be focused only on this material.

Fig. 3 gives the Rietveld refinement results of $LiNi_{0.2}Mn_{0.2}Co_{0.6}O_2$ sample using $[Li_{1-z}Ni_z]_{3a}[Ni_{0.2-z}Mn_{0.2}Co_{0.6}]_{3b}[O_2]_6$ structural model whereas Table 2 summarizes the main structural parameters obtained from this refinement. The little difference between calculated/experimental patterns and the low agreement parameters values (R_{wp}, R_p, R_B) demonstrate that it is a successful refinement. It is important to note that this fitting was obtained for the presence of 0.01 Ni^{2+} ions in the Li plane. A practically ideal

Table 2
Structure parameters of $LiNi_{0.2}Mn_{0.2}Co_{0.6}O_2$ sample prepared at 900 °C for 1 h.

$LiNi_{0.2}Mn_{0.2}Co_{0.6}O_2$ (900 °C/1 h); R_p = 15.6%; R_{wp} = 11.6%; R_B = 3.23%						
Atom	Site	x	y	z	Occupancy	B_{iso} (Å^2)
Li	3a	0	0	1/2	0.990(2)	1.118(4)
Ni2	3a	0	0	1/2	0.010(2)	1.118(4)
Ni1	3b	0	0	0	0.190(2)	0.315(5)
Co	3b	0	0	0	0.6	0.315(5)
Mn	3b	0	0	0	0.2	0.315(5)
O	6c	0	0	0.2593(4)	1	0.274(7)

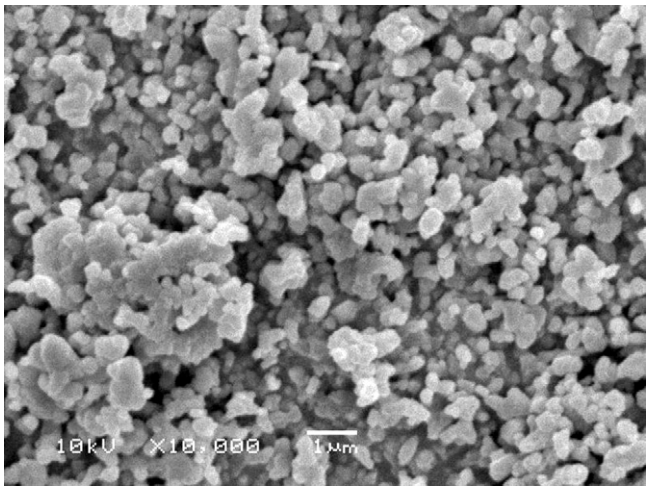

Fig. 4. SEM picture of $LiNi_{0.2}Mn_{0.2}Co_{0.6}O_2$ compound.

2D structure is adopted by the studied $LiNi_{0.2}Mn_{0.2}Co_{0.6}O_2$ cathode material. The amount of the obtained Li/Ni cation disorder is relatively lower than those obtained for $LiNi_{1/3}Mn_{1/3}Co_{1/3}O_2$ [11] and $LiNi_{0.5}Mn_{0.5}O_2$ [12] homologous phases belonging to the same $Li(Ni_xMn_xCo_{1-2x})O_2$ solid solution. This point is very important as the cation mixing in the layered oxides deteriorates significantly their electrochemical performances.

In order to observe the morphology of the $LiNi_{0.2}Mn_{0.2}Co_{0.6}O_2$ material, SEM measurements were carried out. As shown in Fig. 4, the particle sizes seem to be globally uniform. The average size was found to be ~175 nm in diameter. This value agrees with that deduced from the Scherrer's method calculations.

3.3. Magnetic study

Magnetic measurements have been proven to be a sensitive and powerful experimental technique to detect the presence and the amount of the Li/Ni disorder [13,14]. The magnetic behaviour of the studied compound is given in Fig. 5. For temperatures above 45 K, a paramagnetic behaviour was evidenced. The magnetic moment calculated from the Curie–Weiss part of the χ^{-1} vs. T curve is 2.182 μ_B which is in excellent agreement with that calculated in the hypothesis assuming the existence of Mn^{4+} (S = 3/2; $\mu_{Mn^{4+}}$ = 3.87 μ_B), Ni^{2+}

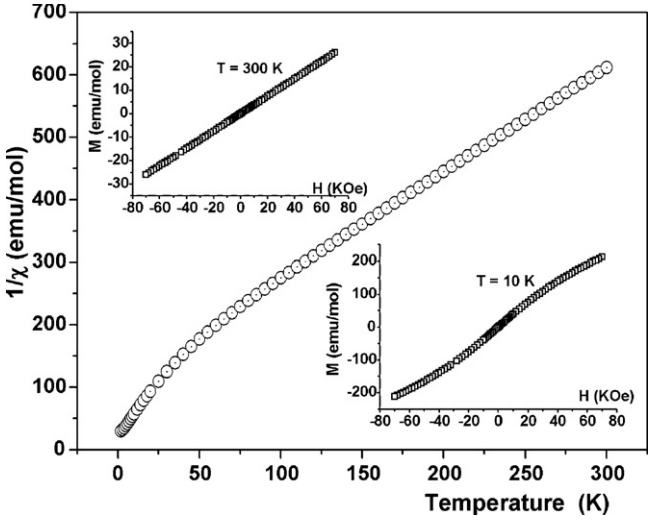

Fig. 5. Thermal variation of the inverse molar susceptibility of $LiNi_{0.2}Mn_{0.2}Co_{0.6}O_2$ oxide. The insets show magnetization vs. applied field at 10 and 300 K.

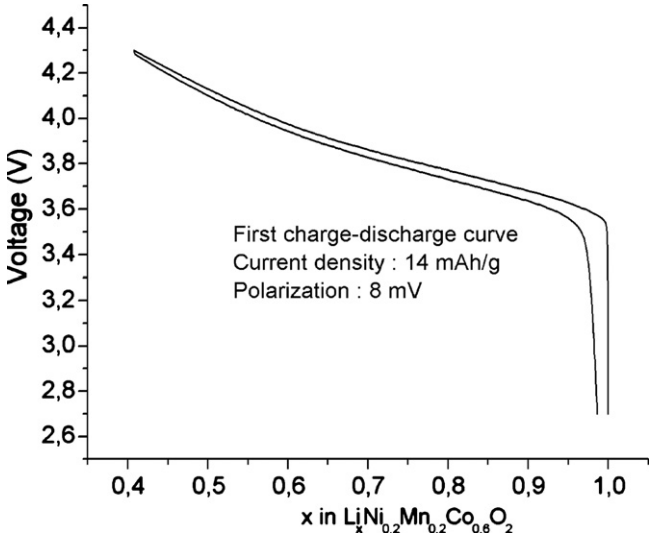

Fig. 6. First charge–discharge cycle of the Li//$Li_xNi_{0.2}Mn_{0.2}Co_{0.6}O_2$ electrochemical cell cycled at C/20 rate between 2.7 and 4.3 V.

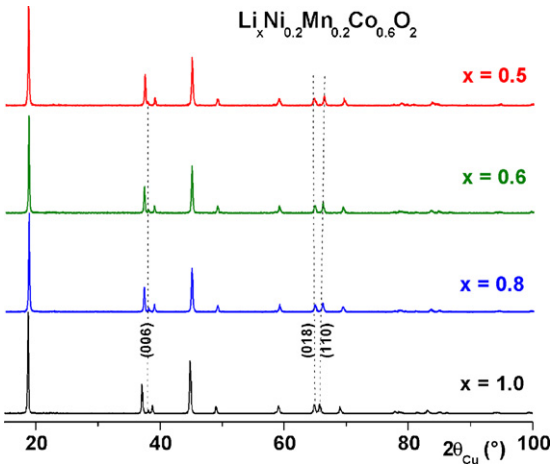

Fig. 7. Ex situ X-ray diffraction patterns for the chemically delithiated $Li_xNi_{0.2}Mn_{0.2}Co_{0.6}O_2$ phases as a function of lithium amount (x).

($S=1$; $\mu_{Ni^{2+}}=2.83\,\mu_B$) and Co^{3+} ($S=0$; $\mu_{Co^{3+}}=0\,\mu_B$) ions. Indeed, the value of the effective magnetic moment was calculated using the following equation: $\mu_{calc.}=[0.2\ (\mu_{Ni^{2+}})^2+0.2\ (\mu_{Mn^{4+}})^2+0.6\ (\mu_{Co^{3+}})^2]^{1/2}=2.147\,\mu_B$.

The oxidation states of these transition metal ions and their individual effective magnetic moments agree well with the literature [15,16].

The M vs. H measurement at 10 K yields a curve with an s-type shape showing neither saturation nor hysteresis. The absence of hysteresis gives a clear indication of good stoichiometry in the $LiNi_{0.2}Mn_{0.2}Co_{0.6}O_2$ sample, with small cationic mixing, as confirmed by the Rietveld refinement ($z=0.01$) and low random distribution of Ni^{2+} and Mn^{4+} on the 3a and 3b sites, respectively [17].

The magnetic behaviour of the layered oxide containing magnetically active transition ions is known to be complicated [18,19]. We have recently demonstrated that a possible spin disordered and magnetically frustrated state arising from competing ferromagnetic (FM) 90° Ni–O–Ni and Mn–O–Mn intralayer interactions and antiferromagentic (AFM) 180° Ni–O–Ni interlayer and 90° Ni–O–Mn intralayer interactions [15,16].

For the studied $LiNi_{0.2}Mn_{0.2}Co_{0.6}O_2$ cathode material, the obtained θ_p temperature was negative ($\theta_p=-62$ K). This indicates that AFM interactions are dominating although the weak amount of extra nickel ions in the Li layer responsible of the strong 180° Ni–O–Ni AFM interlayer superexchange interactions.

3.4. Electrochemistry

Electrochemical characterization was carried out by galvanostatic charge–discharge cycling within 2.7–4.3 voltage window at various C/n rates. Fig. 6 gives the first charge–discharge curve of $LiNi_{0.2}Mn_{0.2}Co_{0.6}O_2$ cathode material at C/20 rate. A good reversibility of the lithium extraction/insertion was evidenced with very low polarization, given by the difference between charge and discharge curves. This suggests that this sample exhibits low impedance due to the small particle size. Furthermore, the irreversible capacity was quite low indicating good capacity retention of the studied sample.

The monotonous evolution of the potential vs. the lithium amount suggests that the redox mechanism involved in the Li//$Li_xNi_{0.2}Mn_{0.2}Co_{0.6}O_2$ electrochemical cycling takes place without structural transitions. Indeed, $LiNi_{0.2}Mn_{0.2}Co_{0.6}O_2$ starting material contains approximately 0.2 Ni^{2+}; 0.2 Mn^{4+} and 0.6 Co^{3+} ions. As Mn^{4+} ions are electrochemically inactive, the only working redox couples are Ni^{2+}/Ni^{4+} and Co^{3+}/Co^{4+}. According to previous works, it was established that Ni ions are preferentially oxidized compared to Co^{3+} during the charge process [20]. It should be noticed that Ni^{2+} ions are probably oxidized to Ni^4 via Ni^{3+}.

Thus, it is believed that the charge process of the Li//$Li_xNi_{0.2}Mn_{0.2}Co_{0.6}O_2$ electrochemical cell begins by the oxidation of Ni^{2+} to Ni^{4+} which involves the extraction of 0.4 lithium ions. The Co^{3+}/Co^{4+} redox couple is involved for the highly oxidized phases $Li_xNi_{0.2}Mn_{0.2}Co_{0.6}O_2$ ($x<0.6$).

In order to evidence the absence of structural transitions during the change of the working redox couple from Ni^{2+}/Ni^{4+} to Co^{3+}/Co^{4+}, XRD patterns of chemically delithiated $Li_xNi_{0.2}Mn_{0.2}Co_{0.6}O_2$ phases were recorded and plotted in Fig. 7.

As shown, the rhombohedral symmetry of the pristine phase (S.G. R-3m) was preserved during the lithium extraction with a slight evolution of the unit cell parameters as evidenced by the progressive splitting of the (0 1 8)/(1 1 0) doublet with lithium extraction. As generally observed in the layered oxides, an expansion of the $c_{hex.}$ parameter and a decrease of the $a_{hex.}$ parameter were detected. The loss of interslab cohesion and the increase of slab covalency upon lithium extraction are responsible for this structural evolution. Thus, this result clearly demonstrated that there is no structural change occurring the electrochemical cycling of the Li//$Li_xNi_{0.2}Mn_{0.2}Co_{0.6}O_2$ cell. Indeed, by reviewing the most studied layered cathode materials, it was established that the initial α-$NaFeO_2$ type structure of $LiMO_2$ oxides transforms irreversibly to spinel structure upon cycling leading to a considerable deterioration of the electrochemical performances [21,22]. This phenomenon was first reported for $LiNiO_2$ [23] which was attributed to the Ni^{4+} migration from the slab to the interslab for the deeply delithiated phases. It appears that for the above-mentioned layered oxide, the irreversible layered-spinel transition is related to the $Ni^{3+}\rightarrow Ni^{4+}$ oxidation reaction. It seems that in the studied sample $LiNi_{0.2}Mn_{0.2}Co_{0.6}O_2$, the absence of Ni^{3+} in its initial state explains the reason for which no structural transition was detected. This point needs to be more explored.

Fig. 8 gives the evolution of the capacity vs. the cycle number during the first 50 cycles between 2.7 and 4.3 V at C/5, C/2, C and 2C rates. Except for the first cycle, the capacity retention is excellent even for the faster rate. As reported in Table 3, while the capacity

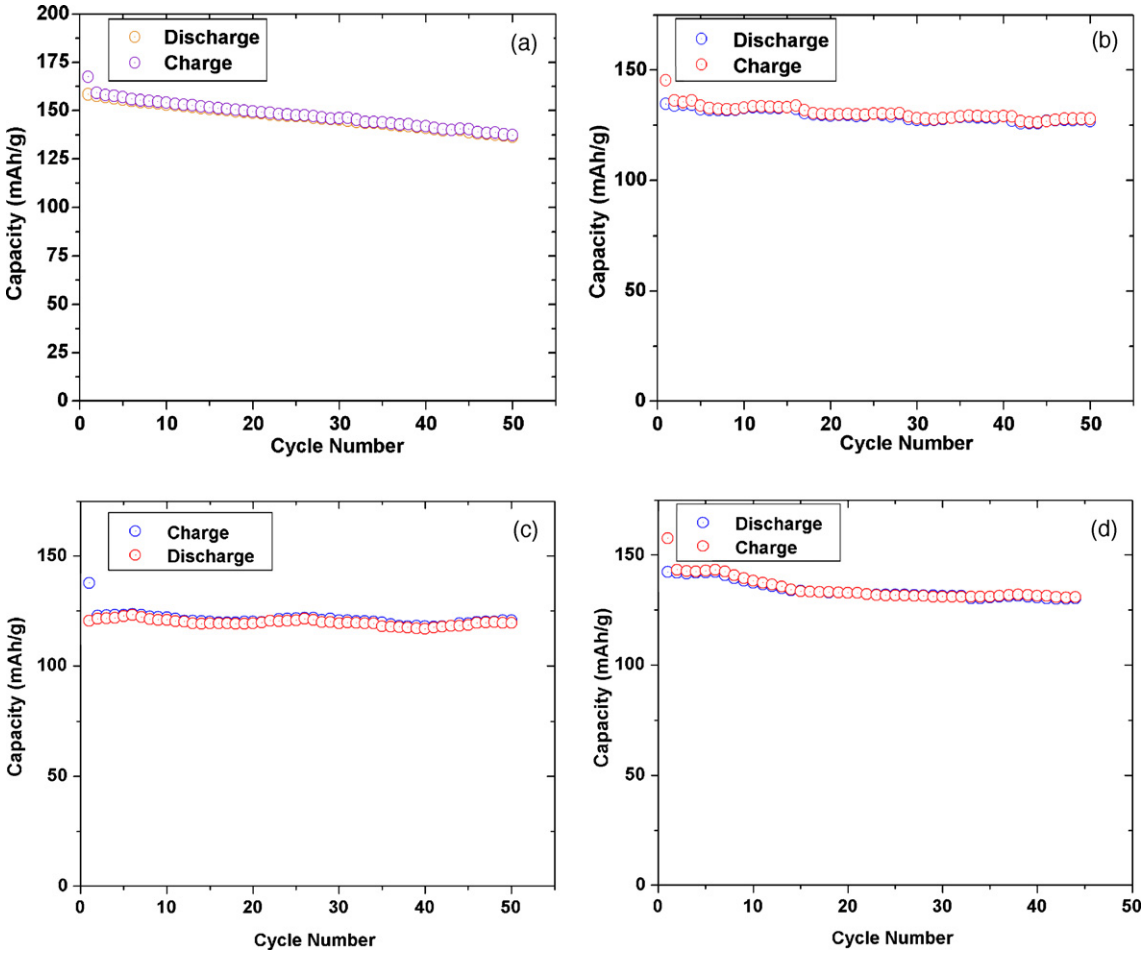

Fig. 8. Charge–discharge capacities for the Li||$LiNi_{0.2}Mn_{0.2}Co_{0.6}O_2$ cell during 50 cycles at various electrochemical rates in the potential range 2.7–4.3 V. (a) C/5, (b) C/2, (c) C and (d) 2C.

Table 3
Comparison of the charge and discharge capacities of $LiNi_{0.2}Mn_{0.2}Co_{0.6}O_2$ cycled at different rates between 2.7 and 4.3 V.

C rates	1st cycle		10th cycle		20th cycle		30th cycle		40th cycle	
	$Q_{cha.}$	$Q_{disch.}$	$Q_{cha.}$	$Q_{disch.}$	$Q_{cha.}$	$Q_{disch.}$	$Q_{cha.}$	$Q_{disch.}$	$Q_{cha.}$	$Q_{disch.}$
C/5	167.8	158.6	154.2	153.1	149.5	148.9	146.1	145.6	141.9	141.1
C/2	146	135.6	132.9	132.8	130.2	130	128	127.6	129.3	129.2
C	138	121.2	123.2	121	120.4	120	120.8	119.5	118.4	117.2
2C	157.6	143	138.4	137.2	133.6	133.5	131.3	131.2	131.2	131

retention is equal to 94.5% for the 1st cycle at C/5 rate, it becomes close to 99% in the following cycles. These electrochemical performances have become higher for the C/2, C and 2C rates. For instance, the capacity fading during 40 cycles is less than 3.3% for the 1C rate which seems to be the optimal regime to use this material as cathode in the lithium batteries. These cycling performances are probably related to the weak amount of the Ni in the lithium plane. This enhances the lithium diffusion in the interslab plane even at relatively high regime.

By comparison with the samples prepared by Jiang et al. [24] by four methods, our sample presents less Li/Ni mixing. The best performances obtained by these authors are attributed to the material prepared by the co-precipitation method, followed by firing the obtained mixture at 550 °C for 3 h then the temperature was ramped to 900 °C for 3 h. Thus, one can conclude that good electrochemical performances could be obtained from sample prepared by combustion method in only one step firing at 900 °C for only 1 h.

4. Conclusions

In order to optimize the synthesis conditions of $LiNi_{0.2}Mn_{0.2}Co_{0.6}O_2$ prepared from the raw mixture obtained by the combustion method, the DTA analysis and the thermal evolution of the XRD patterns were carried out. It has been revealed that this layered compound could be obtained at 900 °C for 1 h. Rietveld refinement of the XRD data evidenced that the formula of this cathode material is: $[Li_{0.99}Ni_{0.01}]_{3a}[Ni_{0.19}Mn_{0.2}Co_{0.6}]_{3b}[O_2]_{6c}$, with almost an ideal α-$NaFeO_2$ type structure. Almost no Ni^{2+} ions are present in the lithium plane which could be considered as quite beneficial for lithium extraction/insertion reactions.

SQUID measurements confirm the existence of Ni^{2+}, Co^{3+} and Mn^{4+} ions and also the predominance of the anti-ferromagnetic interactions ($\theta_p = -62$ K). The oxidation states of the transition metal ions agree well with those generally obtained in the Li(Ni,Mn,Co)O_2 system. Ni^{4+}/Ni^{2+} and Co^{4+}/Co^{3+} are thus the work-

ing redox couples during the lithium extraction/insertion reactions while Mn^{4+} ions remain inactive.

Good reversibility of the charge/discharge process with very low polarization was revealed during the cycling of the $Li//LiNi_{0.2}Mn_{0.2}Co_{0.6}O_2$ electrochemical cell, during which no structural changes were evidenced. Indeed, XRD examination of the chemically delithiated $Li_xNi_{0.2}Mn_{0.2}Co_{0.6}O_2$ ($0.5 \leq x \leq 1.0$) shows that the rhombohedral symmetry was preserved during lithium extraction which induces an evolution from the Ni^{4+}/Ni^{2+} working couple for $0.6 \leq x < 1.0$ to the Co^{4+}/Co^{3+} for $x < 0.6$. The retention of a stable layered oxide framework is believed to contribute to the excellent electrochemical stability of this positive electrode.

Electrochemical tests of the studied cathode, performed in the 2.7–4.3 V window, with different current rates, show that the obtained initial discharge capacity was superior to 158 mAh g^{-1}. The capacity retention in the case of C/5 regime is very high (more than 95%). The same performances are recorded for the faster rates. Nevertheless, the discharge capacity at 1C regime is surprisingly lower than that of 2C. This behaviour could be related to the possible cathode–electrolyte interaction which is reduced when the electrochemical tests are conducted at faster regime. Furthermore, the capacity retention at C/5 rate is relatively worst compared to the other studied regime. This point needs be more clarified. Except these anomalies, the obtained electrochemical performances compete with those of the commercial $LiCoO_2$ and $LiNi_{1/3}Co_{1/3}Mn_{1/3}O_2$ cathodes.

Acknowledgements

The authors gratefully thank University Cadi Ayyad Marrakech (Morocco) and Tokyo University of Science (Japan) for the financial support and Dr H. Sakurai (NIMS, Japan) for the SQUID measurements.

References

[1] T. Ohzuku, Y. Makimura, Chem. Lett. 30 (2001) 744.
[2] Z. Lu, D.D. MacNeil, J.R. Dahn, Solid State Lett. 6 (2001) A191.
[3] Y. Koyama, N. Yabuuchi, I. Tanaka, T. Ohzuku, J. Electrochem. Soc. 151 A (2004) 1545.
[4] N. Yabuuchi, Y. Koyama, N. Nakayama, T. Ohzuku, J. Electrochem. Soc. 152 (2005) A1434.
[5] M.G. Kim, H.J. Shin, J.H. Kim, S.H. Park, Y.K. Sun, J. Electrochem. Soc. 152 (2005) A1320.
[6] T. Ohzuku, Y. Makimura, Chem. Lett. (2001) 642.
[7] J. Li, J.M. Zheng, Y. Yang, J. Electrochem. Soc. 154 (2007) A427.
[8] S.T. Myung, A. Ogata, K.S. Lee, S. Komaba, Y.K. Sun, H. Yashiroa, J. Electrochem. Soc. 155 (2008) A374.
[9] J. Rodriguez-Carvajal, Laboratoire Léon Brillouin (CEA-CNRS), http://www-llb.cea.fr/fullweb/powder.htm.
[10] A.L. Patterson, Phys. Rev. 56 (1939) 978.
[11] Y.J. Shin, M.J. Choi, Y.S. Chang, S. Yoon, K.S. Ryu, S.H. Chang, Solid State Ionics 177 (2006) 515.
[12] A. Abdelg-Ghani, K. Zaghib, F. Gendron, A. Mauger, C.M. Julien, Electrochim. Acta 52 (2007) 4092.
[13] E. Chappel, M.D. Nunez-Regueiro, G. Chouteau, A. Sulpice, C. Delmas, Solid State Commun. 119 (2001) 83.
[14] M. Ma, N.A. Chernova, B.H. Toby, P.Y. Zavalij, M.S. Wittingham, J. Power Sources 165 (2007) 517.
[15] I. Saadoune, M. Dahbi, M. Wikberg, T. Gustafsson, P. Svedlindh, K. Edström, Solid State Ionics 178 (2008) 1668.
[16] M. Dahbi, M. Wikberg, I. Saadoune, T. Gustafsson, P. Svedlindh, K. Edström, Electrochim. Acta 54 (2009) 3211.
[17] H. Kobayashi, H. Sakabe, H. Kageyama, K. Tatsumi, Y. Arachi, T. Kamiyama, J. Mater. Chem. 13 (2003) 590.
[18] A. Rougier, C. Delmas, G. Chouteau, J. Phys. Chem. Solids 57 (1996) 1101.
[19] E. Chappel, M.D. Nunez-Regueiro, S. De Brion, G. Chouteau, V. Bianchi, D. Caurant, N. Baffier, Phys. Rev. B 66 (2002) 132412.
[20] I. Saadoune, M. Ménétrier, C. Delmas, J. Mater. Chem. 7 (2) (1997) 2505.
[21] G. Vitins, K. West, J. Electrochem. Soc. 144 (1997) 2587.
[22] Y.I. Jang, B. Huang, Y.-M. Chiang, D.R. Sadoway, Electrochem. Solid-State Lett. 1 (1998) 13.
[23] M.G.S.R. Thomas, W.I.F. David, J.B. Goodenough, P. Groves, Mater. Res. Bull. 20 (1985) 1137.
[24] J. Jiang, K.W. Eberman, L.J. Krause, J.R. Dahn, J. Electrochem. Soc. 152 (2005) A1874.